Content Based Image Retrieval of T2 Weighted Brain MR Images Similar to T1 Weighted Images

Abraham Varghese[1], Kannan Balakrishnan[2], Reji R. Varghese[3], and Joseph S. Paul[4]

[1] Adi Shankara Institute of Engineering and Technology, Kalady, Kerala
[2] Cochin University of Science and Technology, Cochin, Kerala
[3] Co-Operative Medical College, Cochin, Kerala
[4] Indian Institute of Information Technology and Management, TVM, Kerala

Abstract. Magnetic Resonance images play a crucial role in the diagnosis and management of the diseases of the brain. The MRI can acquire cross sectional images of our body, based on T1 and T2 relaxation of the tissues. As the information presented in these two images is often complimentary, both these images need to be compared for accurate clinical diagnosis. Hence automatic retrieval of similar slices of T1 weighted images from T2 weighted images or vice versa is of much value. In this paper T2-weighted (or T1 weighted) similar brain MR images within and across the subjects are retrieved using T1-weighted (or T2 weighted) as query images. The rotational and translational invariant form of Modified Local Binary Pattern is used to retrieve the similar anatomical structure MR images.

1 Introduction

The advantage of Magnetic Resonance Imaging (MRI) over other imaging modalities persuade radiologist to relies on MRI to study various brain related problems. Unlike Computer Tomography (CT), Single Photon Emission Computed Tomography (SPECT), and Positron Emission Tomography (PET), MRI operates at radio-frequency (RF) range; thus there is no ionizing radiation involved. Furthermore, MRI can generate excellent soft tissue contrast, and has the capability of producing images at any orientation. Moreover the information content present in MR images is extremely rich compared to other imaging modalities. After a magnetized spin system is perturbed from its equilibrium condition by an RF pulse, it will return to the equilibrium after a sufficient time once the perturbation is removed [1]. The recovery of longitudinal component is called T1 relaxation while the decay of transverse magnetization is called T2 relaxation. In the diagnosis process, radiologist depends on both T1 and T2 weighted images as the information presented in the two images is complementary. As the number of digital images produced is increasing in an alarming rate due to advancements in various imaging technologies, retrieving T2(or T1) images corresponds to T1(or T2) is challenging. A very popular approach of image retrieval

P. Maji et al. (Eds.): PReMI 2013, LNCS 8251, pp. 474–481, 2013.

is to first annotate the images by text and then use text-based database management systems (DBMS) to perform image retrieval [2,3,4,5,6]. But the difficulties such as subjectivity of human perception, amount of labour required etc faced by the manual annotation approach became more and more acute due to the emergence of large collection of images. To overcome these difficulties Content Based Image Retrieval (CBIR) was proposed. CBIR is any technology that helps to organize digital pictures by their visual content. The term CBIR appears in the literature in early 1990s in connection with retrieving images from a large database using color and shape features [7]. The term has since been widely used to describe the process of retrieving desired images from a large collection on the basis of features such as color, texture, shape etc which are extracted automatically from the images themselves [8,9,10,11]. Using the low level features, some of the CBIR systems such as QBIC[12], Photobook[13],Virage[14], VisualSEEK[15], Netra[16], SIMPLIcity[17] were developed.
In this paper similar anatomical T1 and T2 weighted images are retrieved using a texture descriptor Local Binary Pattern (LBP). The LBP is modified by incorporating local variance information into it and is termed as Modified Local binary Pattern(MOD-LBP).

2 Methodology

The overview of the image retrieval scheme is shown in Fig 1. The MOD-LBP image code is computed using a circular neighborhood with radius R and P neighborhood pixels. The MOD-LBP image is converted to polar form(r,θ) in order to compensate for rotation and translation in spatial description of the features by taking centroid as the origin of the image. The output image obtained is of size $\boldsymbol{N} \times \boldsymbol{N}$ with N points along the r-axis and N points along the θ-axis. The pixel value at the non-integer coordinate of the image is estimated using bilinear interpolation. The histogram of MOD-LBP is computed spatially, where the entries of each bin are indexed over annularly angularly partitioned regions. The pixel intensities are brought in the range [0, L], where L is a positive integer and normalized histogram of the image is taken as feature vectors for similarity computation. The images in the database are ranked based on the Bhattacharya distance between query and database images. The average rank and accuracy is calculated for a set of query images.

2.1 Pre processing

The image is converted to binary image by applying suitable thresholding. The components (objects) that have fewer than P(say) pixels are removed from the binary image, resulting only one connected component. The centroid of the binary image is computed using REGIONPROPS operation, which measures a set of properties for each connected component (object) in the binary image. Then resulting image is multiplied with original image for further feature extractions.

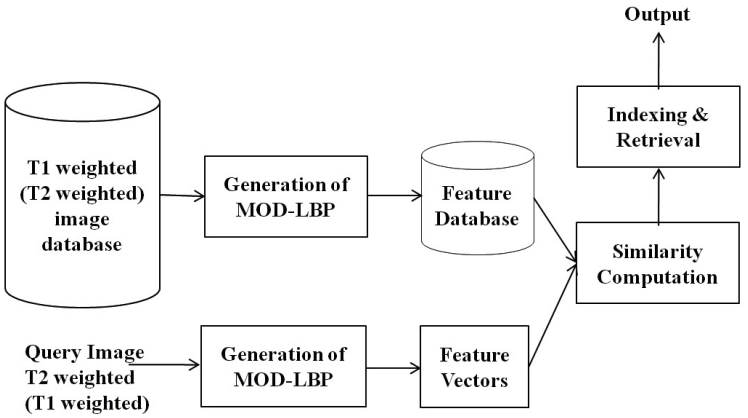

Fig. 1. Block diagram of Image retrieval scheme

2.2 LBP and MOD-LBP

The Local Binary Pattern (LBP) operator is a gray-scale invariant texture primitive, derived from a general definition of texture in a local neighborhood. Due to its discriminative power and computational simplicity, the LBP operator has become a highly popular approach in various computer vision applications, including visual inspection, image retrieval, remote sensing, biomedical image analysis, biometrics, motion analysis, environment modeling, and outdoor scene analysis, etc. LBP is formed by comparing gray value of center pixel (gc) with that of P neighborhood pixels in the local neighborhood [18,19].

$$LBP = \sum_{i=0}^{P-1} s(g_i - g_c)2^i \qquad (1)$$

The operator $LBP_{P,R}$, is derived based on a symmetric neighbor set of P members gi (i = 0, 1, P-1) within a circular radius of R. The signs of the differences Eq (1) in a neighborhood are interpreted as a P -bit binary number, resulting in 2^P distinct values for the LBP code. One way to eliminate the effect of rotation is to perform a bitwise shift operation on the binary pattern P-1 times and assign the LBP value that is the smallest, which is now referred to as $LBP^{ri}_{P,R}$.The above measure is invariant to monotonic gray level changes because just the sign of the differences only are considered instead of their exact values. In order to account for the changes in contrast and rotational invariance against grayscale shift with respect to the window taken, the definition of the LBP is modified as shown in Eq(2).

$$MOD - LBP(P,R) = \frac{1}{P}\sum_{i=0}^{P-1} s(g_i - g_c)(g_i - \mu)^2 \qquad (2)$$

where μ is the mean of the P circular neighborhood pixels and R is the radius . Bilinear interpolation is applied to the non-integer coordinate points on the

image in order to interpolate the pixels. The weights are assigned to the P-bit binary pattern based on the square of the gray scale difference between neighborhood pixel values and mean gray scale value. The resultant image is formed by assigning the decimal equivalent of the weighted binary number to the central pixel. As MOD-LBP is computed locally, it is invariant to monotonic gray level change, and it can even resist intra-image illumination variation as long as the absolute gray value differences are not much affected. Normalized histogram of MOD-LBP is taken as feature vector and Bhattacharya distance is used for similarity computation

3 Results

The slices (T1 and T2 weighted) used in this work, are acquired on a 1.5 Tesla, General Electric(GE) Signa HDxt MR Scanner from Pushpagiri Medical College Hospital, Tiruvalla, Kerala, India. Axial, 2D, 5mm thick slice images, with a slice gap of 1.5mm are acquired with the field-of-view (FOV) of range 220mm to 250mm. The T2 (TR/TE(eff.) of 3500-4500/ 85-105(eff.)ms) images are collected using Fast Spin Echo (FSE) sequences with a matrix size of 320 X 224 (Frequency X Phase) and a NEX (Averages) of 2. The T1 weighted images (TR/TE of 450-550/8-12ms) were acquired using standard spin echo (SE) sequence with a matrix size of 288 X 192 (Frequency X Phase) and a NEX(Averages) of 2.

We have categorized unregistered Brain MR images of different subjects into 4 levels, for independently evaluating the performance of the histogram based image retrieval method.
L1- the foramen magnum (The cerebellum with paranasal sinus is present)
L2- Above the fourth ventricle (Caudate nucleus, thalamus, basal ganglia are seen)
L3- mid ventricular section
L4- above the ventricle. In order to test the robustness of MOD-LBP with respect to intensity variations simulated bias fields from the BrainWeb MR simulator (20 and 40) are used [20]. These bias fields provide smooth variations of intensity across the image. As the MOD-LBP is calculated locally, intensity inhomogeniety has less sensitivity on it because the bias field in MRI is locally smooth. The degree of dissimilarity between MOD-LBP of original and the degraded images (100 images randomly chosen) are computed using the Bhattacharyya distance, $d = 1 - \sum_{i=0}^{L_1-1} \sqrt{p(i)q(i)}$ where p and q are normalized histograms with L1-bins. The mean dissimilarity scores fall in the range of [0 1], where 0 means that all original images and its degraded images are perfectly similar. Table 1 shows the effect of bias field in similarity computation between original image and degraded image using Bhattacharya distance. It is observed that the MOD-LBP computation helps to decrease dissimilarity between original and degraded image. Also as bias field increases the dissimilarity increases and MOD-LBP with window size 3 and 5 shows more or less same dissimilarity.Table 2 shows the time taken for MOD-LBP computation over different window size .

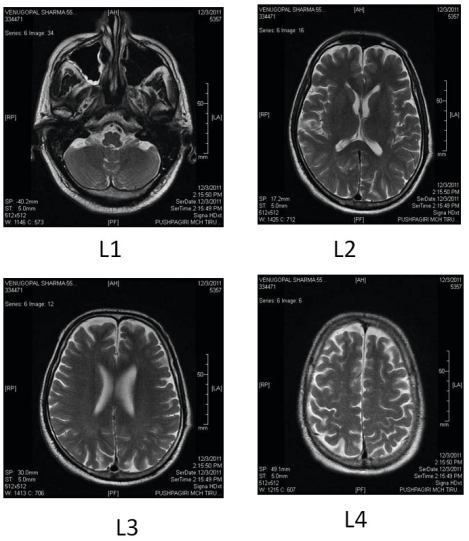

Fig. 2. Different classes of T2 weighted axial MR slices

3.1 Retrieval of T2 Weighted Images Similar to T1 Weighted Image across the Subjects

In order to test the performance of the retrieval system we had taken 40 T2 weighted images from L1, 32 images from L2, 32 images from L3 and 40 images from L4 as query image across the subjects and calculated average rank and accuracy of retrieving similar T1 weighted images based on the histogram of different LBP variants. An average rank, which shows the closeness of the system performance, is calculated using the formula,

$$Rank = \frac{1}{N_R}\left(\sum_{i=1}^{N_R} R_i - \frac{N_R(N_R-1)}{2}\right) \quad (3)$$

N_R represents number of relevant images and Ri represents the rank at which the ith relevant image is retrieved [21]. The Accuracy of the retrieval system for a set of queries is also calculated using the formula,

$$Acc = \left(1 - \frac{No{:}of irrelevant images retrieved}{Total no{:}of images}\right) \times 100 \quad (4)$$

Table 3 illustrates the comparison of LBP and MOD-LBP in retrieving first 6 relevant images. It reveals that the MOD-LBP performs better in terms of average rank and accuracy for retrieving first 6 relevant images

3.2 Single Subject Performance

In order to study the retrieval performance evaluation in a single subject scenario, the most similar image corresponds to a given query from same subject data is retrieved. As our database consists of 20 slices of 20 subjects data, with four landmark slices per subject, there are 204 query images. For a query image i, the images in the database are ranked based on the distance value between

Table 1. The dissimilarity score between original and degraded image

Method	*WindowSize*	*BiasField*	
		20	40
Histogram		8.36×10^{-2}	12.26×10^{-2}
$MOD - LBP(8,1)$	3	4.93×10^{-2}	8.68×10^{-2}
$MOD - LBP(16,2)$	5	4.93×10^{-2}	8.83×10^{-2}

Table 2. Time taken for MOD-LBP computation over different window size

Operator	$Time(S)$
$MOD - LBP(8,1)$	$0.686s$
$MOD - LBP(16,2)$	$1.809s$

Table 3. The average rank and accuracy of retrieving first 6 T2 weighted images using T1 as query image

Class	*Method*	*Measure*	1	2	3	4	5	6
	LBP	*MeanRank*	2.07	3.10	3.98	4.93	5.87	6.93
*L*1		*Accuracy*	99.41	98.26	97.37	96.22	95.22	93.74
	MOD	*MeanRank*	2.93	3.43	4.02	4.55	4.99	5.47
	$-LBP(16,2)$	*Accuracy*	98.93	98.37	97.67	97.15	96.81	96.19
	LBP	*MeanRank*	3.80	5.43	8.02	10.85	13.71	16.46
*L*2		*Accuracy*	98.49	96.74	93.44	90.14	87.03	84.30
	MOD	*MeanRank*	2.93	3.97	4.71	5.43	6.40	7.26
	$-LBP(16,2)$	*Accuracy*	98.96	97.85	97.20	96.45	95.02	94.34
	LBP	*MeanRank*	3.67	5.10	5.98	7.08	8.16	9.30
*L*3		*Accuracy*	98.58	97.06	96.42	95.00	93.90	92.55
	MOD	*MeanRank*	1.80	2.33	2.84	3.38	3.92	4.42
	$-LBP(16,2)$	*Accuracy*	99.57	99.01	98.48	97.87	97.30	96.84
	LBP	*MeanRank*	1.13	1.27	1.33	1.37	1.43	1.51
*L*4		*Accuracy*	99.93	99.78	99.74	99.74	99.63	99.48
	MOD	*MeanRank*	1.0	1.07	1.11	1.15	1.23	1.29
	$-LBP(16,2)$	*Accuracy*	100	99.93	99.89	99.85	99.70	99.67

query and database image. The error in the retrieval of images correspond to ith query image is defined as $Err(i) = \sum_{j=1}^{K-1} |S_j - S_k|$ where Sj is the slice number at rank j, and k is the rank of the relevant slice. The retrieval error of the system is the mean of Err. Table 3 shows the mean retrieval error in retrieving relevant images. The results show that the retrieval error is minimum when the query and target images belong to the same class.

Table 4. Time taken for MOD-LBP computation over different window size .Mean retrieval error of retrieving relevant images a) Mean error of retrieving T2 weighted images using T2 weighted image as query b) Mean error of retrieving T1 weighted images using T1 weighted image as query c) Mean error of retrieving T1 weighted images using T2 weighted image as query.

	(a)	(b)	(c)
$LBP(8,1))$	11.72	8.25	22.68
$LBP(16,2)$	11.95	11.66	24.26
$MOD-LBP(8,1)$	5.66	3.13	16.9
$MOD-LBP(16,2)$	2.22	2.8	13.85

4 Conclusion

The paper illustrates a method to retrieve T2 weighted axial images from T1 weighted images and vice versa. The result reveals the robustness of local measure to intensity related problems. The method is applied to retrieve images from a single subject data as well as data across the subjects which would help the expert in the decision-diagnosis process. As the method is rotational and translational invariant, the costlier registration can be avoided and it is very easy to compute. The method can be extended to retrieve coronal and sagittal slices. An optimum performance can be achieved using proper relevance feed mechanism.

References

1. Einstein, A.: On the movement of small particles suspended in stationary liquids required by the molecular-kinetic theory of heat. Annalen der Physik 17, 549–560 (1905)
2. Bloch, F.: Nuclear induction. Physical Review 70, 460–474 (1946)
3. Chang, N.S., Fu, K.S.: A Relational Database System for Images. Technical Report TR-EE 79-28, Purdue University (May 1979)
4. Chang, N.S., Fu, K.S.: Query-by pictorial-example. IEEE Trans. on Software Engineering SE-6(6) (1980)
5. Chang, S.K.: Pictorial data-base systems. IEEE Computer (1981)
6. Chang, S.K., Hsu, A.: Image information systems: Where do we go from here? IEEE Trans. on Knowledge and Data Engineering 4(5) (1992)
7. Chang, S.K., Yan, C.W., Dimitroff, D.C., Arndt, T.: An intelligent image database system. IEEE Trans. Software Eng. 14(5) (1988)

8. Kato, T.: Database architecture for content-based image retrieval in Image Storage and Retrieval Systems. In: Jambardino, A.A., Niblack, W.R. (eds.) Proc. SPIE, vol. 1662, pp. 112–123 (1992)
9. Algrain, P., Zhang, H., Petkovic, D.: Content-based representation and retrieval of visual media, A review of the state-of-the-art. Multimed. Tools Appl. 3(3), 179–202 (1996)
10. Rui, Y., Huang, T., Chang, S.F.: Image retrieval: Current techniques, promising directions and open issues. J. Visual Commun. Image Represent. 10(1), 39–62 (1999)
11. Smeulders, A.W., Worring, M., Santini, S., Gupta, A., Jain, R.: Content-based image retrieval at the end of the early years. IEEE Trans. Pattern Anal. 22(12), 1349–1380 (2000)
12. Snoek, C.G.M., Worring, M.: Multimodal video indexing: A review of the state-of-the-art. Multimed. Tools Appl. 25(1), 535 (2005)
13. Faloutsos, C., Barber, R., Flickner, M., Hafner, J., Niblack, W., Petkovic, D., Equitz, W.: Efficient and effective querying by image content. J. Intell. Inf. Syst. 3(34), 231–262 (1994)
14. Pentland, A., Picard, R.W., Scaroff, S.: Photobook: Content-based manipulation for image databases. Int. J. Comput. Vision 18(3), 233–254 (1996)
15. Gupta, A., Jain, R.: Visual information retrieval. Commun. ACM 40(5), 70–79 (1997)
16. Smith, J.R., Chang, S.F.: VisualSeek: A fully automatic content based query system. In: Proceedings of the Fourth ACM International Conference on Multimedia, pp. 87–98 (1996)
17. Ma, W.Y., Manjunath, B.: Netra: A toolbox for navigating large image databases. In: Proceedings of the IEEE International Conference on Image Processing, pp. 568–571 (1997)
18. Wang, J.Z., Li, J., Wiederhold, G.: SIMPLIcity: semantics-sensitive integrated matching for picture libraries. IEEE Trans. Pattern Anal. Mach. Intell. 23(9), 947–963 (2001)
19. Ojala, T., Pietikainen, M., Maeenpaa, T.: Multiresolution gray-scale androtation invariant texture classification with local binary patterns. IEEE Trans. Pattern Anal. Mach. Intell. 24(7), 971–987 (2002)
20. Unay, D., Ekin, A., Jasinschi, R.: Medical image search and retrieval using local binary patterns and KLT feature points. In: Proc. Int. Conf. Image Process., pp. 997–1000 (2008)
21. `http://www.bic.mni.mcgill.ca/brainweb/`
22. Muller, H., Muller, W.: Automated Benchmarking in Content Based Image Retrieval, work supported by Swiss National Foundation for Scientific Research (grant no. 2000-052426.97)